Pournazarian, Bahram; Saeedian, Meysam; Lehtonen, Matti; Taheri, Shamsodin; Pouresmaeil, Edris

# Microgrid Stability Analysis Considering Current State-Feedback

*Published in:*
Proceedings of the 11th IEEE International Symposium on Power Electronics for Distributed Generation Systems, PEDG 2020

*DOI:*
10.1109/PEDG48541.2020.9244320

Published: 01/01/2020

*Document Version*
Peer-reviewed accepted author manuscript, also known as Final accepted manuscript or Post-print

# Microgrid Stability Analysis Considering Current State-Feedback

Bahram Pournazarian, Meysam Saeedian
*Department of Electrical Engineering and Automation*
*Aalto University*
Espoo, Finland
firstname.lastname@aalto.fi

Matti Lehtonen
*Department of Electrical Engineering and Automation*
*Aalto University*
Espoo, Finland
matti.lehtonen@aalto.fi

Shamsodin Taheri
*Département d'informatique et d'ingénierie*
*Université du Québec en Outaouais*
Gatineau (Quebec), Canada
shamsodin.taheri@uqo.ca

Edris Pouresmaeil
*Department of Electrical Engineering and Automation*
*Aalto University*
Espoo, Finland
edris.pouresmaeil@aalto.fi

***Abstract*—A converter-based microgrid including several distributed generations (DG) and energy storage systems (ESS) embodies a small power system consisting of several synchronous machines and loads. The stability issue and the coordination between generating units is an essential challenge, either in island or in grid-connected microgrids. The instability of individual DGs cause the microgrid instability as a whole. So, the individual unit stability and the microgrid stability both must be ensured simultaneously. The state feedback concept which is considered in control of converters has a substantial effect on the converter stability and microgrid stability, subsequently. This study will introduce a small-signal model for the microgrid including converter-based DGs and loads considering the previous studies in this field. A phase locked loop (PLL) is required for the control strategy. The effect of current state feedback is scrutinized and analyzed in this study as the main contribution. The effectiveness of the proposed control strategy to enhance the microgrid stability using chosen state feedback is examined through simulation studies. The simulation results ensure that the microgrid stability using the proposed control method and state-feedback is strengthened.**

***Index Terms*—Microgrid, small-signal stability, state feedback, island operation.**

**Nomenclature**

| | |
|---|---|
| *DG* | Distributed Generation |
| *ESS* | Energy Storage System |
| *HVDC* | High-Voltage Direct Current |
| *MG* | Microgrid |
| *PLL* | Phase-Locked Loop |
| *RES* | Renewable energy sources |
| *THD* | Total Harmonic Distortion |
| *ROCOF* | Rate of change of frequency |
| *Nadir* | Point of minimum frequency |
| *F* | current state-feedback factor |
| *LPF* | Low-pass filter |
| *PCC* | Point of common coupling |

## I. Introduction

### A. Motivation and Background

The worldwide concern over future energy resources and global warming crisis motivates the movement towards full-electrical vehicles, microgrids and smart grids supplied by renewable energy sources (RES). A cheap and carbon-free source of energy provided by solar cells, wind farms and the other renewable energy sources are typical prime movers for future full-electrical applications. Similar to a conventional power system including various machine-based units, the stability analysis is necessary for new and low-inertia microgrids [1]. The microgrid small-signal stability analyzed in [2] was a milestone for microgrid stability analysis. The advanced researches such as [3] optimize the virtual impedances based on small-signal stability analysis. However, the phase locked loop (PLL) as a necessary unit to control and coordinate several DGs in the MG must be taken into account, either comparing the units phases to the phase of one local DG or have a central phase reference [4]. Moreover, the state-feedback concept which is one of the control methodologies can change the eigenvalues of a system and enhance its stability.

### B. Relevant Literature

Supplying the demand load and controlling the voltage and frequency are two critical procedures in an island MG which have been done using different control methods [5]. The hierarchical control platform in [6] includes stable, precautionary and emergency zones and evaluates the permitted intervals for control parameters using eigenvalues analysis. The graph theory was applied in [7] to study the integration of new DGs into a MG and the effect of inappropriate DG allocation on MG stability was scrutinized. A non-linear large-signal mathematical model for a MG including dc-side dynamics was developed in [8] which was applied to draw

the stability domain. The research in [9] reports that cascading lead compensators in power-frequency control loop can extend the stability margin of an island MG. The distributed control framework in [10] evaluates the small-signal stability based on local data receiving from nearby buses, if the MG is prone to instability, some sparse communication links are applied among a group of buses to enhance the MG stability. A thorough small-signal stability study of an inverter-based MG including a PLL is found in [11] which controls the converters in *dq* reference frame. The MG clustered as several MGs in connection which others are modeled and analyzed in [12] which optimizes the MG cluster controller parameters based coupling among MGs and low-damping modes drawn from small-signal stability analysis. The small-signal MG modeling in [13] includes communication latency effect which is necessary for distributed primary and secondary control. It is reported in [14] that the internal model-based excel the conventional PI-based voltage and current controllers to make the MG stable. An equal or non-equal load-sharing in an hybrid MG (including inverter-based DGs and diesel generators) could influence on MG dynamic stability as reported in [15].

### C. Contributions and Organization

As a part of our current study on microgrids stability and control, the evaluation of the effect of current state-feedback on microgrid small-signal stability is the main interest of this study. A PLL unit is considered for the converters which can affect the stability of island microgrid. The control methodology is implemented on all converters in an island microgrid and a common phase angle is dictated to all of them to have a common *dq* reference frame. The effect of changing the current state-feedback factor on different characteristics of a microgrid is analyzed. A thorough simulation study comes afterwards to examine the effect of the proposed control strategy and the proposed current state-feedback factor. The rest of this paper is arranged so as follows; Section II describes the island microgrid control methodology, Section III explains the microgrid small-signal stability. The simulation and results are drawn and analyzed in section IV. In section V conclusions of this study are presented.

## II. The Island Microgrid Control Methodology

An island MG including several DGs, ESS and loads operates like a miniature power system composed of several synchronous generators and loads. The former is controlled based on droop-based voltage and frequency characteristics, the later applies governors with speed-droop characteristic on synchronous generators to realize stable load sharing among generating units [1]. Controlling the DGs on a a common *dq* frame is the dual concept of the angle coordination between rotors. Any converter adjusts its *dq* frame angle with the common *dq* frame. A typical converter-based DG connected to the PCC is demonstrated in Fig.1. The DG is supposed to deliver a fixed DC voltage to the converter. The output LC filter including a damping resistor ($R_d$) is connected to the output terminal. The output terminal voltages ($V_{o-abc}$) and currents ($I_{o-abc}$) are measured continuously as seen in Fig.1. The converter controller is demonstrated inside a dashed-box in Fig.1. A well-known *dq* transformation is used as seen in similar research works [2]. Different control blocks are illustrated subsequently.

### A. Power calculator

The instantaneous power components are computed by *dq* voltages and currents as depicted in Fig.1. Subsequently, the real and reactive powers provided by a converter are calculated as the outputs of low-pass filters.

$$p = \frac{3}{2}(v_{od}.i_{od} + v_{oq}.i_{oq}) \Rightarrow P = \frac{\omega_c}{s+\omega_c}.p \tag{1}$$

$$q = \frac{3}{2}(v_{od}.i_{oq} - v_{oq}.i_{od}) \Rightarrow Q = \frac{\omega_c}{s+\omega_c}.q \tag{2}$$

### B. Droop control

The conventional droop equations are applied to control the voltage and frequency of the island MG. It is worth mentioning that the considered *dq* frame is such a way that the *d*-axis voltage is forced to zero.

$$\omega^* = \omega_0 - m_p \times (P - P_0) \tag{3}$$

$$v_{od}^* = 0 \tag{4}$$

$$v_{oq}^* = v_{oq0} - n_q \times (Q - Q_0) \tag{5}$$

### C. Voltage controller

The voltage controller can include a current state-feedback as seen in [19] which is a recent study on MG voltage and frequency control. The PLL model introduced in [11] is applied and it is not repeated here because of page limits. $\omega_{PLL}$ is the angular frequency measured by the PLL. The current state feedback is multiplied by $F$ which is named as current state feedback coefficient and later in this study its effect on MG stability will be examined.

$$\dot{\phi_d} = \omega_{PLL} - \omega^* \Rightarrow i_{ld}^* = F.i_{od} + k_{iv}.\phi_d + k_{pv}.\dot{\phi_d} \tag{6}$$

$$\dot{\phi_q} = v_{oq}^* - v_{oq} \Rightarrow i_{lq}^* = F.i_{oq} + k_{iv}.\phi_q + k_{pv}.\dot{\phi_q} \tag{7}$$

### D. Current controller

As it can be seen in Fig.1 the pre-filtering currents are fed into the current controller to adjust the voltage commands in *dq* frame accordingly.

$$\dot{\gamma_d} = i_{ld}^* - i_{ld} \Rightarrow v_{id}^* = -\omega_n.L_f.i_{lq} + k_{ic}.\gamma_d + k_{pc}.\dot{\gamma_d} \tag{8}$$

$$\dot{\gamma_q} = i_{lq}^* - i_{lq} \Rightarrow v_{iq}^* = -\omega_n.L_f.i_{ld} + k_{ic}.\gamma_q + k_{pc}.\dot{\gamma_q} \tag{9}$$

### E. Control on a common dq frame

It is well-known that for a power system including several synchronous generators, the angle of one rotor is chosen as the reference in order to coordinate the units generation and keep the whole system stable [1]. The dual rule is that in a

MG including several converters and machines, the frequency of one converter's voltage could be chosen as an angular frequency for a common phase-frame. All the local variables are translated into global phase-frame. This concept was well-described in previous researches [2], [4]. The conversion matrix for changing local values into global values on a common reference frame is as follows:

$$\begin{bmatrix} f_D \\ f_Q \end{bmatrix}_{common} = \begin{bmatrix} cos(\delta_{com}) & -sin(\delta_{com}) \\ sin(\delta_{com}) & cos(\delta_{com}) \end{bmatrix} \begin{bmatrix} f_d \\ f_q \end{bmatrix}_{local} \quad (10)$$

Apparently, the inverse transformation holds for translating common values into local values such as bus voltages. It should be noted that the term $\delta_{com}$ for any converter in the transformation matrix is the difference between the angle of d-axis of that converter local reference frame and the angle of the d-axis of common reference frame.

## III. Microgrid small-signal stability

The dynamic equations describing a MG are mainly non-linear. Some research has been focused on the linearization of these equations around an operating point [2], [11]. It is noteworthy that the bus voltage components are output variables and using the virtual resistor method they are defined as a function of currents which are state variables. The sign $\pm$ is applied because for any line a current direction is assumed. So, the sign will be minus for one bus and it will be plus for another bus while using equations 11,12. $v_{bD}$ and $v_{bD}$ are bus voltage components on common *DQ* reference frame.

$$v_{bD} = r_N(i_{od} \pm i_{line_d} - i_{load_d}) \quad (11)$$

$$v_{bQ} = r_N(i_{oq} \pm i_{line_q} - i_{load_q}) \quad (12)$$

Considering the current state-feedback will change the small-signal equations introduced in [11]. The first step is to choose state-variables for the 2-bus MG. The state-variables for the MG are:

$$\begin{aligned} x = [&\Delta\delta_1, \Delta P_1, \Delta Q_1, \Delta\varphi_{d1}, \Delta\varphi_{q1}, \Delta\gamma_{d1}, \Delta\gamma_{q1}, \Delta i_{ld1}, \\ &\Delta i_{lq1}, \Delta v_{od1}, \Delta v_{oq1}, \Delta i_{od1}, \Delta i_{oq_1}, \Delta\varphi_{PLL_1}, \Delta v_{odf1}, \\ &\Delta\delta_2, \Delta P_2, \Delta Q_2, \Delta\varphi_{d2}, \Delta\varphi_{q2}, \Delta\gamma_{d2}, \Delta\gamma_{q2}, \Delta i_{ld2}, \Delta i_{lq2}, \\ &\Delta v_{od2}, \Delta v_{oq2}, \Delta i_{od2}, \Delta i_{oq2}, \Delta\varphi_{PLL2}, \Delta v_{odf2}, \Delta i_{load_{d1}}, \\ &\Delta i_{load_{q1}}, \Delta i_{load_{d2}}, \Delta i_{load_{q2}}, \Delta i_{line_d}, \Delta i_{line_q}] \end{aligned}$$

where the indices 1 and 2 refer to converters 1 and 2 state variables respectively.

$$\dot{x} = Ax \quad (13)$$

The state matrix (A) for a two-buses MG including two converters and two local loads located on buses and a line between two buses is a 36×36 matrix linearized around an operating point $(x_0)$. As the state-space equations are mentioned in [11] while the current state-feedback was ignored, the modified entries in A matrix are clarified, for other state-equations the reference [11] is available.

A(6,12)=F
A(7,13)=F

TABLE I
THE CONTROLLERS AND MICROGRID PARAMETERS.

| Parameter | Value | Parameter | Value |
|---|---|---|---|
| $L_f$ | 4.2 $mH$ | $r_f$ | 0.50 Ω |
| $L_c$ | 0.5 $mH$ | $r_c$ | 0.09 Ω |
| $C_f$ | 15$\mu F$ | $R_d$ | 2.025 Ω |
| $\omega_c$ | 50.26 $rad/s$ | $\omega_n$ | 377 $rad/s$ |
| $\omega_{c,PLL}$ | 7853.98 $rad/s$ | $\omega_{PLL}$ | 377 $rad/s$ |
| $m$ | 0.001 $rad/Ws$ | $n$ | 0.001 $V/Var$ |
| $r_N$ | 1000 Ω | $Voq_n$ | 85.0 $V$ |
| $R_{load1}$ | 25 Ω | $L_{load1}$ | 15 $mH$ |
| $R_{load2}$ | 25 Ω | $L_{load2}$ | 7.5 $mH$ |
| $R_{pert1}$ | 25 Ω | $L_{pert1}$ | 7.5 $mH$ |
| $R_{line}$ | 0.15 Ω | $L_{line}$ | 0.4 $mH$ |
| $v_{bD1}$ | 0 V | $V_{bQ1}$ | 85 $V$ |
| $v_{bD2}$ | 0 V | $V_{bQ2}$ | 85 V |
| $kp_{pll}$ | 0.25 | $ki_{pll}$ | 2 |
| $kp_v$ | 0.5 | $ki_v$ | 25 |
| $kp_c$ | 1 | $ki_c$ | 100 |
| $P_0$ | 0 | $Q_0$ | 0 |

A(8,12)=$L_f^{-1}$ × kpc × F
A(9,13)=$L_f^{-1}$×kpc×F
A(10,12)=-$C_f^{-1}$-$R_d$ × $L_c^{-1}$ × $(-r_c - r_N)$+$R_d$ × $L_f^{-1}$ × kpc ×F
A(11,13)=-$C_f^{-1}$-$R_d$× $L_c^{-1}$ ×$(-r_c - r_N)$+$R_d$ × $L^{-1}$×kpc×F
A(21,27)=F
A(22,28)=F
A(23,27)=$L_f^{-1}$×kpc×F
A(24,28)=$L_f^{-1}$×kpc×F
A(25,27)=-$C_f^{-1}$-$R_d$× $L_c^{-1}$ ×$(-r_c - r_N)$+$R_d$× $L_f^{-1}$×kpc×F
A(26,28)=-$C_f^{-1}$-$R_d$×$L_c^{-1}$ ×$(-r_c - r_N)$+$R_d$ × $L_f^{-1}$×kpc×F

## IV. Simulation results

The simulation studies were implemented on a 2-buses MG introduced in [11]. For the sake of simplicity, full MG specifications are listed in Table.I. The serial $R_{pert} = 25\Omega$ and $L_{pert} = 7.5$ mH are switched-in at time= 1.8 seconds in bus 1. Prominent characteristics of the MG are scrutinized in order to examine the effect of current state-feedback factor on them. In order to analyze the small-signal of the MG which is a nonlinear system, the state-space equations are linearized around an operating point which is:

$$\begin{aligned} x_0 = [&0, 418.18, 76.104, 0.0034, 0.13152, 0.0014, 0.8656, \\ &0.1198, 3.287, 0.0414, 84.92, 0.5996, 3.2813, -0.2088, \\ &0.0427, 0.0003, 415.95, 70.12, 0.00153, 0.1308, 0.0012, \\ &0.8656, 0.071, 3.2716, 0.04243, 84.929, 0.5514, 3.2659, \\ &-0.208, 0.042, 0.749, 3.2113, 0.4011, 3.3359, 0.15028, \\ &-0.0699] \end{aligned}$$

### A. Microgrid eigenvalues

While changing the state-feedback factor (F), the major eigenvalues of the MG are plotted accordingly. Fig.3 demonstrates the major eigenvalues of the test MG while the state-

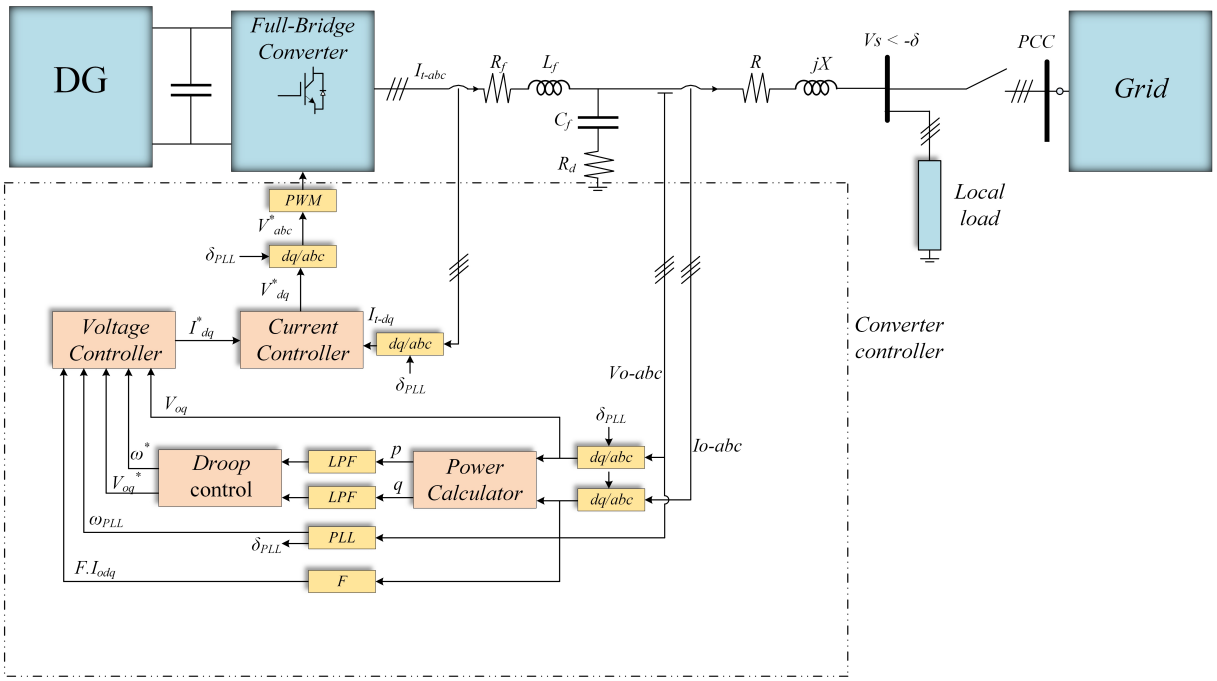


Fig. 1. The proposed control method for a converter in an island microgrid.

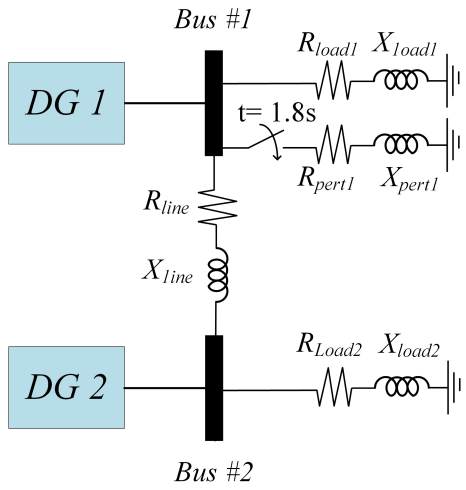


Fig. 2. The effect of changing current state-feedback factor (F) on the microgrid eigenvalues.

feedback factor (F) is changing from zero to infinity. It is noteworthy that those values of 'F' which cause the MG to become unstable are not of our interest, but the boundary of instability. As the figure shows, for a specific interval $(0 < F < 0.53)$ increasing this factor enhances the MG stability by making the real-part of the eigenvalues more negative. For another interval $(0.53 < F < 0.76)$, by increasing the state-feedback factor the MG stability has deteriorated. From the MG stability point of view, the optimal value for $F$ is 0.53.

### B. Microgrid reference frequency

The reference frequency for any inverter is calculated using Eq.3. This reference frequency is dictated to the pulse-width modulation unit. As the applied scenario was to add active and reactive loads to bus 1, according to the Eq.3, the reference

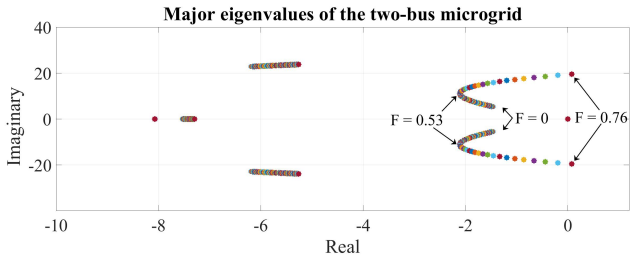


Fig. 3. The effect of changing current state-feedback factor (F) on the microgrid eigenvalues.

frequency will decrease. Fig.4 demonstrates frequency characteristics for the MG under study for three different cases with different state-feedback factors (F=0, 0.53 and 0.76). For the case F=0.76 which is the bound to instability, the undamped oscillations in the reference frequency in Fig.4 are visible (light-blue curve). So, apparently a big value of state-feedback factor could deteriorate the MG stability. Comparing the frequency references for $F$=0 and 0.76 in Fig.4 clarifies that the magnitudes of oscillations are almost similar. However, the settling time for a case with $F = 0.76$ is smaller which can be accounted for as an advantage.

### C. Microgrid measured frequency

As the frequency is a global parameter, it will have a unique value over a microgrid in the steady-state. So, a PLL is enough for measuring the frequency in the small MG under study. Apparently, for a bigger MG dispersed over a vast area, the communication delay will make the situation different and several PLL units in all remote areas are required. The droop coefficients for both inverters are chosen as equal. The frequency Nadir for a case with $F = 0.76$ is the worst case

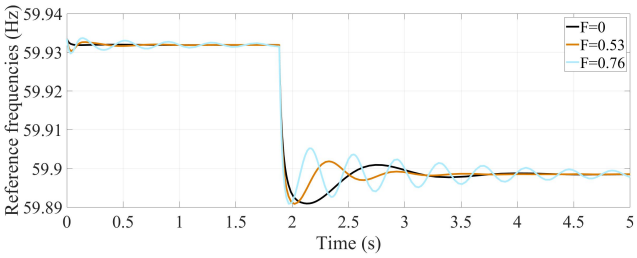


Fig. 4. The microgrid reference frequency for three different current state-feedback factors, $F = 0$; $F = 0.53$; $F = 0.76$.

and for a case with $F = 0.53$ is the best value. On the other hand, the ROCOF for a case with $F = 0.53$ is the lowest value.

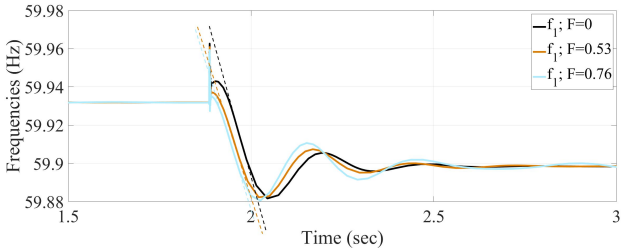


Fig. 5. The microgrid frequency for three different current state-feedback factors, $F = 0$; $F = 0.53$; $F = 0.76$.

### D. Microgrid voltage components

Fig.6 demonstrates the *dq* components of voltages at MG buses for three scenarios with different current state-feedback factors ($F$= 0, 0.53 and 0.76). The d-axis voltage in all cases is supposed to become zero in steady-state based on the control method. The d-axis voltage for a case with $F = 0.76$ has long-standing oscillations which is because the MG is in the instability boundary. For both cases with $F = 0$ and $F = 0.53$ the voltage fluctuations are damped, however the magnitude of these oscillations for a case with F=0.53 is lower than the case with $F = 0$, so $F = 0.53$ is preferable. The q-axis voltages which are controlled at nominal values are seen in bottom part of Fig.6. It is seen that increasing the F factor from 0 to 0.53 enhances the transient voltage performance, for the case with $F = 0.76$, the q axis voltage is higher but the d-axis is was oscillating. Consequently, the preferable value for current state-feedback is $F = 0.53$.

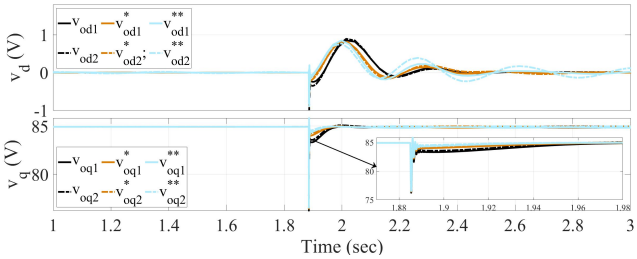


Fig. 6. The *dq* voltage components of buses in three different cases, $F = 0(v_{od}, v_{oq})$; $F = 0.53(v^*_{od}, v^*_{oq})$; $F = 0.76(v^{**}_{od}, v^{**}_{oq})$.

### E. The active and reactive powers

The real and reactive powers supplied by converters 1 and 2 are plotted simultaneously in Fig.7 by normal line and dashed line, respectively. The active powers for converters 1 and 2 reach at an identical value in the steady state because of having similar droop coefficients. So, the active power injected by converter 1 is analyzed here (normal lines at topper part of Fig.7). It is seen that by increasing $F$ from 0 to 0.53, the rise time decreases and the active power reaches at its steady-state value after 0.5 second, but for the case with F=0 it approximately after 1 second reaches at its steady-state value. However, for the case with $F = 0.76$ the long-standing oscillations are seen in the active power of both converters which is definitely undesired. So, from the point of view of active power, the preferred value is $F = 0.53$.
The reactive powers injected by two inverters are seen in the bottom part of Fig.7. Apparently, the reactive powers generated by two converters are not equal, because a traditional reactive power-voltage droop control was applied. Similarly, while the $F$ factor is increased from 0 to 0.53 the reactive power response becomes faster and reaches at its final value at a shorter time. But for the case with $F = 0.76$ the undamped fluctuations in reactive power are seen which is not acceptable. All in all, from the reactive power point of view, the optimal value is $F = 0.53$.

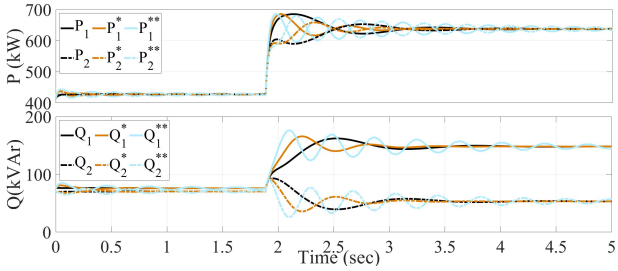


Fig. 7. The real and reactive powers generated by two converters in three different cases, $F = 0(P, Q)$; $F = 0.53(P^*, Q^*)$; $F = 0.76(P^{**}, Q^{**})$.

### F. Microgrid output current components

The *dq* current components injected by converters 1 and 2 are demonstrated in Fig.8 with normal line and dashed line, respectively. The d-axis current is the dual of reactive power and the q-axis is the dual of active power according to the control method. In the steady-state both converters generate identical q-axis currents. While the current state-feedback factor ($F$) is increased from 0 to 0.53 the current response becomes faster (brown curve in bottom Fig.8) and the settling time decreases. But if the factor is further increased to $F = 0.76$, the current turns out to be fluctuating as the MG is in the boundary of instability. The d-axis current component is seen on the topper part of Fig.8. The converter 1 injects a bigger portion of d-axis current than converter 2, that's because it is nearer to the load-change point. Comparing cases with $F = 0$ and $F = 0.53$, the current response in the case with $F = 0.53$ has a shorter rise-time and settling time. But for the case with $F = 0.76$ the d-axis current response is fluctuating

and the MG is apparently unstable. All in all, from the current response point of view, the preferred value for $F$ is 0.53.

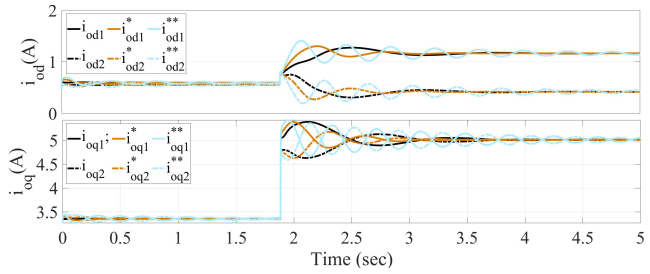


Fig. 8. The output current components injected by two converters in three different cases, $F = 0(i_{od}, i_{oq})$; $F = 0.53(i^*_{od}, i^*_{oq})$; $F = 0.76(i^{**}_{od}, i^{**}_{oq})$.

## V. Conclusions

In this paper, a small-signal model for an inverter-based MG including PLL and current state-feedback ($F$) is developed. The proposed control method is implemented on a 2-bus test MG. First of all, the effect of current state-feedback factor ($F$) on the MG stability is examined. It is seen that there is an optimal value for regarding the MG small-signal stability which is $F = 0.53$ in this study. If the current state-feedback factor is increased further than this optimal value, the MG is propelled into the unstable region. The remaining parts of this study are devoted to analyzing the effect of current state-feedback factor on the MG frequency, voltage, powers and currents. According to the simulations, the ROCOF and Nadir of frequency are enhanced while setting an optimal current state-feedback factor. The voltage losses in case with $F = 0.53$ is lower and the voltage response is faster. But for the case with $F = 0.76$ the voltage shows long-standing oscillations. For the active powers and q-axis currents, the system response has shorter rise time and settling time, both converters inject equal active powers and also q-axis currents in the steady-state which is because droop coefficients are equal. For the reactive powers and the d-axis current components, the reactive power response is faster and the settling time is shorter while having $F = 0.53$ compared to the case with $F = 0$. However, a bigger value like $F = 0.76$ leads to the MG instability. All in all, choosing an optimal current state-feedback factor could enhance the MG stability while providing an excel MG performance.

## References


[1] P. Kundur,, "Power systems stability and control.," *McGraw-Hill,* 1994.

[2] N. Pogaku, M. Prodanovic, and T. C. Green, "Modeling, Analysis and Testing of Autonomous Operation of an Inverter-Based MG," *IEEE Trans. Power Electron.,* vol. 22, no. 2, pp. 613-625, Mar. 2007.

[3] B. Pournazarian, S. S. Seyedalipour, M. Lehtonen, S. Taheri and E. Pouresmaeil, "Virtual Impedances Optimization to Enhance Microgrid Small-Signal Stability and Reactive Power Sharing," *IEEE Access,* vol. 8, pp. 139691-139705, 2020.

[4] B. Pournazarian, E. Pouresmaeil, M. Saeedian, M. Lehtonen, R. Chan and S. Taheri, "Microgrid Frequency & Voltage Adjustment Applying Virtual Synchronous Generator," 2019 International Conference on Smart Energy Systems and Technologies (SEST), Porto, Portugal, 2019, pp. 1-6.

[5] H. Han, X. Hou, J. Yang, J. Wu, M. Su and J. M. Guerrero, "Review of Power Sharing Control Strategies for Islanding Operation of AC MGs," *IEEE Trans. Smart Grid,* vol. 7, no. 1, pp. 200-215, Jan. 2016.

[6] Z. Zhao, P. Yang, J. M. Guerrero, Z. Xu and T. C. Green, "Multiple-Time-Scales Hierarchical Frequency Stability Control Strategy of Medium-Voltage Isolated Microgrid," in IEEE Transactions on Power Electronics, vol. 31, no. 8, pp. 5974-5991, Aug. 2016.

[7] Y. Song, D. J. Hill and T. Liu, "Impact of DG Connection Topology on the Stability of Inverter-Based Microgrids," in IEEE Transactions on Power Systems, vol. 34, no. 5, pp. 3970-3972, Sept. 2019.

[8] M. Kabalan, P. Singh and D. Niebur, "A Design and Optimization Tool for Inverter-Based Microgrids Using Large-Signal Nonlinear Analysis," in IEEE Transactions on Smart Grid, vol. 10, no. 4, pp. 4566-4576, July 2019.

[9] D. K. Dheer, V. A. S, O. V. Kulkarni and S. Doolla, "Improvement of Stability Margin of Droop-Based Islanded Microgrids by Cascading of Lead Compensators," in IEEE Transactions on Industry Applications, vol. 55, no. 3, pp. 3241-3251, May-June 2019.

[10] Y. Song, D. J. Hill, T. Liu and Y. Zheng, "A Distributed Framework for Stability Evaluation and Enhancement of Inverter-Based Microgrids," in IEEE Transactions on Smart Grid, vol. 8, no. 6, pp. 3020-3034, Nov. 2017.

[11] M. Rasheduzzaman, J. A. Mueller and J. W. Kimball, "An Accurate Small-Signal Model of Inverter- Dominated Islanded MGs Using *dq* Reference Frame," *IEEE J. Emer. Sel. Topics Power Electron.,*vol. 2, no. 4, pp. 1070-1080, Dec. 2014.

[12] J. He, X. Wu, X. Wu, Y. Xu and J. M. Guerrero, "Small-Signal Stability Analysis and Optimal Parameters Design of MG Clusters," *IEEE Access,* vol. 7, pp. 36896-36909, 2019.

[13] Y. Yan, D. Shi, D. Bian, B. Huang, Z. Yi and Z. Wang, "Small-Signal Stability Analysis and Performance Evaluation of MGs Under Distributed Control," *IEEE Trans. Smart Grid,* vol. 10, no. 5, pp. 4848-4858, Sept. 2019.

[14] S. Leitner, M. Yazdanian, A. Mehrizi-Sani and A. Muetze, "Small-Signal Stability Analysis of an Inverter-Based MG With Internal Model-Based Controllers," *IEEE Trans. Smart Grid,* vol. 9, no. 5, pp. 5393-5402, Sep. 2018.

[15] A. Aderibole, H. H. Zeineldin, M. S. El-Moursi, J. C. Peng and M. Al Hosani, "Domain of Stability Characterization for Hybrid Microgrids Considering Different Power Sharing Conditions," in IEEE Transactions on Energy Conversion, vol. 33, no. 1, pp. 312-323, March 2018.

[16] M. A. Hassan, "Dynamic Stability of an Autonomous Microgrid Considering Active Load Impact With a New Dedicated Synchronization Scheme," in IEEE Transactions on Power Systems, vol. 33, no. 5, pp. 4994-5005, Sept. 2018.

[17] D. K. Dheer, V. A. S, O. V. Kulkarni and S. Doolla, "Improvement of Stability Margin of Droop-Based Islanded MGs by Cascading of Lead Compensators," *IEEE Trans. Ind. App.,* vol. 55, no. 3, pp. 3241-3251, May-June 2019.

[18] P. Vorobev, P. Huang, M. Al Hosani, J. L. Kirtley and K. Turitsyn, "High-Fidelity Model Order Reduction for Microgrids Stability Assessment," IEEE Trans. Power Syst., vol. 33, no. 1, pp. 874-887, Jan. 2018.

[19] B. Pournazarian, P. Karimyan, G.B. Gharehpetian, M. Abedi, and E. Pouresmaeil,"Smart participation of PHEVs in controlling voltage and frequency of island microgrids,"*Int. J. Elect. Power Energy Syst.,* vol.110, pp. 510-522, 2019.